Experimental Optimization of Nanostructured Nickel Oxide Deposited by Spray Pyrolysis for Solar Cells Application

[1a]Ukoba, O.K, [a]Inambao, F.L. and [a]Eloka-Eboka, A.C.

[a]Discipline of Mechanical Engineering University of KwaZulu-Natal, Durban, 4041, South Africa.

Abstract

This study focused on the experimental optimization of nanostructured nickel oxide (NiO) for solar cell applications. The optimization procedure involved the variation of the precursor concentrations of nickel acetate with attendant measurement of the properties of nickel oxide films. The films were spray deposited on glass substrate. Nickel acetate precursor was used at a substrate temperature of 350 °C. Precursor concentrations were: 0.025 M, 0.05 M, 0.075 M and 0.1 M respectively. The surface morphology revealed nanostructured film with particles densely distributed across the substrate's surface. The films are homogeneous, smooth, well adherent and devoid of pinholes and cracks. The morphology became grainier as the precursor solution increased. Elemental composition exposes the presence of Ni and O elements in NiO film. Oxygen concentration decreases as precursor solution increases. The film structural property reveals that deposited NiO film has an amorphous structure at 0.025 M while the other concentrations are polycrystalline in nature with cubic structure. X-ray diffractometry (XRD) further reveals that the intensity of NiO films increases with increased molarity. Preferred orientation was along the (1 1 1) peak with minor intensity along the (2 0 0) peak. XRD patterns have peak diffraction at ($2\theta = 37$ ° and 43 °) for the (1 1 1) and (2 0 0) planes respectively, and 64 ° for the (2 2 0) plane for 0.1 M. Crystallite size was obtained at 63.77 nm maximum. Film thickness increased with increasing precursor concentration from 6.277 μm to 11.57 μm. Film micro strain was observed to have compression for all precursor solutions. Optical studies showed that transmittance decreased with increasing concentration from 80 % to 71 %. Optical band gap energy was between 3.94 eV to 3.38 eV as precursor concentration increased, revealing the effect of varied concentrations on NiO film properties. Optimized results obtained are precursors in the development of low cost, efficient, durable solar cell fabrication for developing countries.

Keywords: NiO; solar cell material; annealing, low income

INTRODUCTION

The provision of affordable and efficient energy is among the top 50 grand challenges facing humankind in the 21st century [1-2]. Electricity is non-existent for over 20 % of the world's population with developing countries comprising 99.8 % of that number [3]. Sub-Sahara Africa is home to nearly 85 % of the 1.3 billion people living in developing countries without access to electricity [4], with an estimated electrification rate of around 32 % [5]. Several countries in Africa and south Asia lack access to electricity [6], while many countries on those continents have a high degree of electricity supply disruption with an average of less than four hours of power supply daily [7]. However, developed countries like in Europe, America and Asia have turned their fortunes around in terms of electricity generation by harnessing power from renewable energy sources.

Apart from the stable supply of electricity, other attendant challenges still loom in such regions. They include the relatively high cost of electricity, underdeveloped infrastructure especially in remote areas, uneven billing of electricity, high tariffs, and unfavorable policies to mention but a few. This has caused many citizens to resort to alternate sources of electricity supply. Renewable energy has been confirmed as a viable solution to ending global electricity problems as it exceeds world energy demand [8]. Renewable energy is sustainable and not harmful to the environment. Solar energy is a good source of renewable energy [9]. The hourly solar influx on the surface of the earth surpasses annual human energy needs [10]. Solar energy is environmentally benign [11-12]. About 40 % of CO_2 emissions is saved per year for each 1 % of world electricity demand supplied by solar grid [13]. However, high costs are militating against the successful deployment of solar technology worldwide. Solar cells are an integral aspect of solar energy [14].

Large scale production at affordable cost is being studied for the purpose of fabrication of solar cells [15]. Existing methods are not suitable for scaling up due to the expensive nature and complexities associated with the vacuum environment required for fabrication. Nanostructured metal oxide, however, is promising. Nanostructured materials offer potential improvement in solar cells efficiency and reduction in manufacturing and electricity production costs [16] due to the increased surface area to volume ratio of nanoparticles. This makes nanostructured materials more efficient and better energy collectors [17]. Nanostructured materials have unique characteristics that cannot be obtained from conventional macroscopic materials [9]. The drawback of conventional materials is low absorption properties resulting in low efficiency in solar cell devices. Inorganic semiconducting materials are economical, environmentally friendly and viable sources for solar cells [18].

Fabrication of nanostructured metal oxide films is attracting interest in terms of technological applications [19-22]. They have been studied due to their vast range of use [23], including in applications such as solar cells, UV detectors,

electrochromic devices, anti-ferromagnetic layers, p-type transparent conductive thin films, and chemical sensors [24-29]. The properties of metal oxides can be experimentally optimized for better results in a specific application. The properties of the metal oxides are affected by the control of the desired morphology, structure, size and other properties of the material for specific applications [30- 31]. Metal oxides often show n-type conductivity with a few displaying p-type. NiO has p-type conductivity [32]. NiO exists in various oxidation states [33]. It is pale green with a cubic structure. It is durable with stable chemical properties and optical densities. NiO has been prepared using sputtering [34], sol-gel [35], electron beam deposition [36], laser ablation [37], and chemical bath deposition [38]. The spray pyrolysis technique (SPT) allows coating of large areas by films of very thin layers with uniform thickness [39]. SPT has low material cost, is easy to set up and economical for mass production [40-41]. These features informed the application of SPT in this study. Some of the relevant literature has highlighted the potential of SPT in NiO fabrication of solar cells.

A recent review by Ukoba et al. [42] presented the different precursors and their characterization methods for spray deposition of NiO thin film and concluded that the usefulness of SPT as a simple but efficient method cannot be over-emphasized for mass production of solar cells. The review advocated for the exploration of different optimization approaches [42]. The present study is therefore tilted towards the optimization of the precursor concentrations of NiO films and the properties of NiO films as an alternate solar energy material with emphasis on efficiency and affordability. The objectives include: preparing a nanostructured NiO thin film on glass substrate using SPT to deposit an aqueous solution of nickel acetate, and subsequently determining the effects of varying the concentrations of nickel acetate on the properties of NiO films.

EXPERIMENTAL PROCEDURE

Spray Pyrolysis Setup

The experimental configuration used is shown in Fig. 1, comprising air compressor, temperature controller, heater, exhaust fan and pipe, and spray gun with attached container. The container houses the precursor solution. A hose connects the air compressor to the spray gun. A temperature of 350 ℃ was attained and read by a thermocouple attached to the heater before commencing deposition.
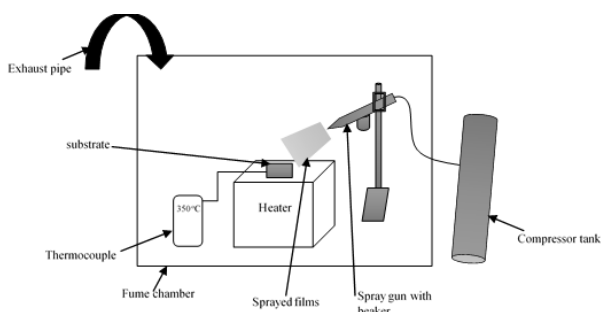

Figure 1: Experimental set-up of Spray pyrolysis technique

Precursor Preparation and Deposition

Precursor solution was nickel acetate tetrahydrate of concentration 0.025 M, 0.05 M, 0.075 M and 0.1 M. This was mixed and stirred in 50 mL distilled water for 10 min. Thereafter the solution was poured into the spray gun container. The glass substrate was chemically and ultrasonically cleaned before usage. The glass substrate was heated at a constant temperature of 350 ℃ on a heater. Other deposition parameters were maintained to obtain uniform film thickness. The optimum deposition parameters of spray deposited NiO film are shown in Table 1. Each droplet is found to be smaller than micro-sized particles. The sprayed solution on the preheated substrate glass experiences evaporation and solute precipitation before pyrolytic decomposition as shown in Equation (1). Nickel oxide is given off as a final product.

$$\text{Ni}(CH_3COO)_2.4H_2O \xrightarrow{heat} NiO + 7H_2O \uparrow + 4CO_2 \uparrow \quad (1)$$

The color of prepared thin film was observed to be gray, uniform and strongly adherent to the glass.

Table 1. Optimum deposition parameter of SPT NiO film

Deposition parameter	Value
Substrate temperature	350 ℃
Distance of spray nozzle to substrate distance	20 cm
Spray rate	1 ml/min
Spray time	1 min
Time between sprays	30 s
Carrier gas	Filled compressed air of 1 bar

Characterization

The morphology of deposited NiO film was studied using a ZEISS ULTRA PLUS Field Emission Gun Scanning Electron Microscope (FEGSEM). Elemental analysis was performed using an Energy Dispersive X-ray Spectrometer (EDX: "AZTEC OXFORD DETECTOR"). Structural properties of the deposited NiO films were investigated using an EMPYREAN (PANalytical) X-ray powder diffractometer for a range of 5 ° to 90 ° 2θ angles. Measured film thickness was compared with calculated film thickness obtained using the weight difference method. Optical properties were studied in wavelengths of 300 nm to 1000 nm with a SHIMADZU UV-3600UV-VIS Spectrometer model.

RESULTS AND DISCUSSION

Morphological Studies

FEGSEM micrographs are represented in Fig. 2. These micrographs reveal homogeneous, smooth, well adherent film devoid of pinholes and cracks. The morphology becomes grainier with bigger flakes with increasing concentration. This is an improvement on results observed by Bari et al. [43] and Sadaati et al.[44]. This confirms that varying the concentration of the precursors affects NiO film morphology.
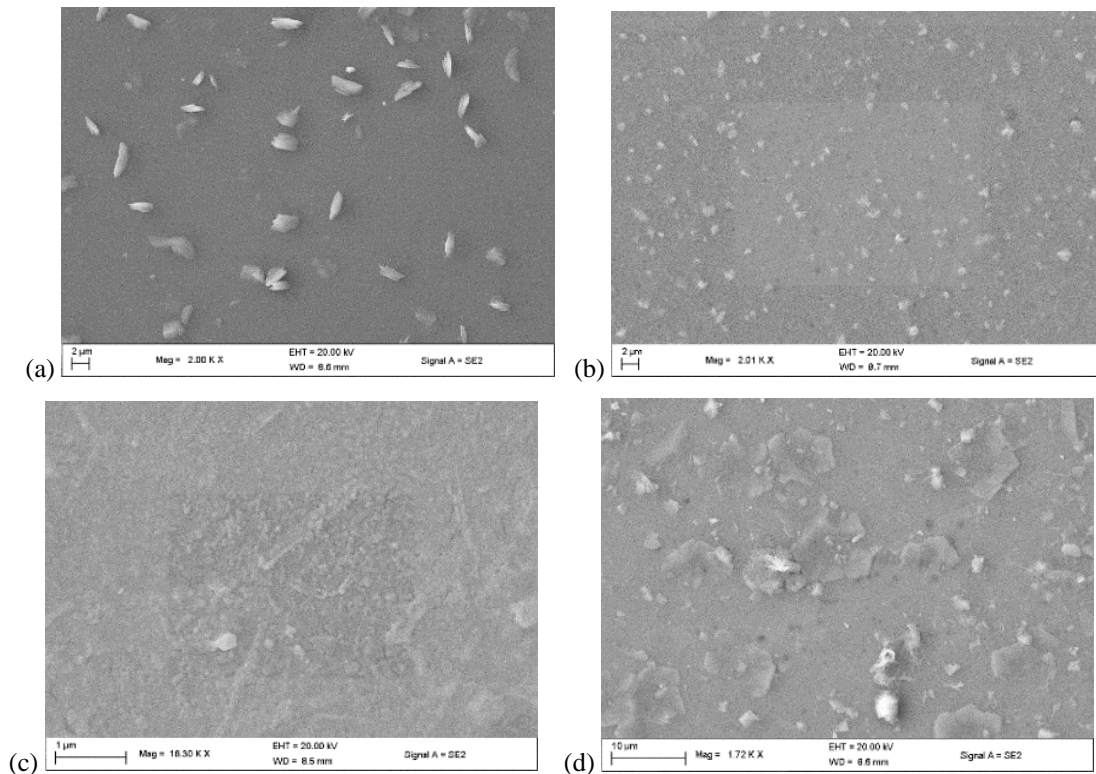
Figure 2: SEM micrographs of nickel oxide (NiO) film on glass substrate at (a) 0.025M and (b) 0.05Mgreen (c) 0.075M and (d) 0.1M

Elemental Composition Analysis

Figure 3 shows the EDX for the different concentrations for the NiO thin films thereby confirming the presence of Ni and O elements in the NiO thin films. Oxygen concentration in deposited NiO films decreases as the precursor concentration increases as seen in the EDX result. This may be due to increased film growth on the glass substrate thereby making less of the glass (oxygen) visible. This gives better distribution of Ni and O compared with a previous reported distribution [45]. An additional silicon (Si) element was also observed. This is because Si is present in soda-lime glass or soda-lime-silica glass substrate [46].

Film Thicknesses and Precursor Solution Concentration

Film thicknesses were considered with precursors of concentration 0.025 M and 0.1 M. The film thickness was obtained using SEM cross sectional profiling as shown in Fig. 4 and the weight difference method expressed in Equation (2) [47] and plotted in Fig. 5.

$$t = \frac{m}{A\rho} \tag{2}$$

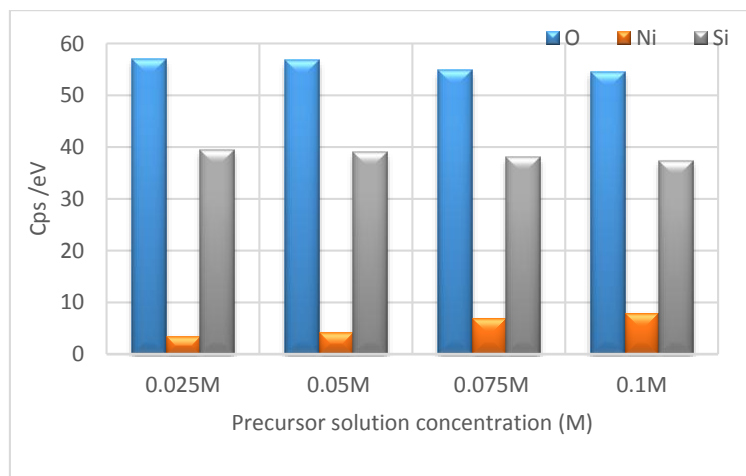Where t is film thickness, m is actual mass deposited, A is thin film area and ρ is density of material.

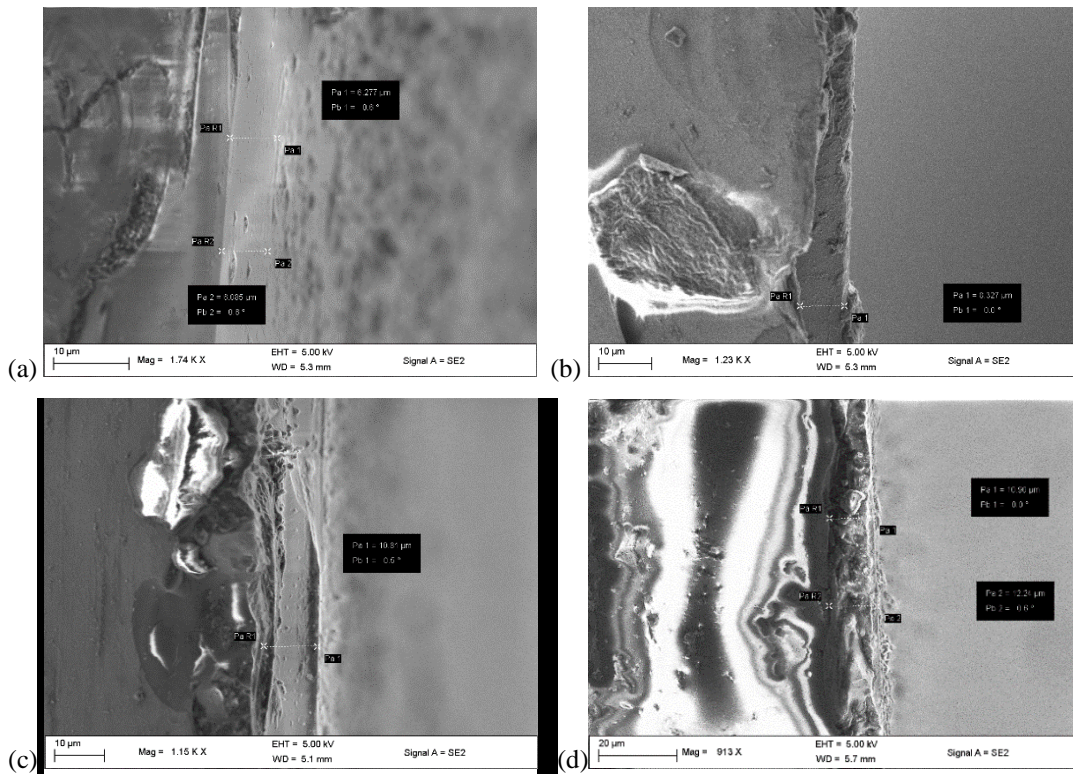**Figure 3:** Elemental composition of deposited NiO films

Figure 4. Film thickness obtained from SEM cross-sectional profiling for (a) 0.025M; (b) 0.05M; (c) 0.075M; (d) 0.1M
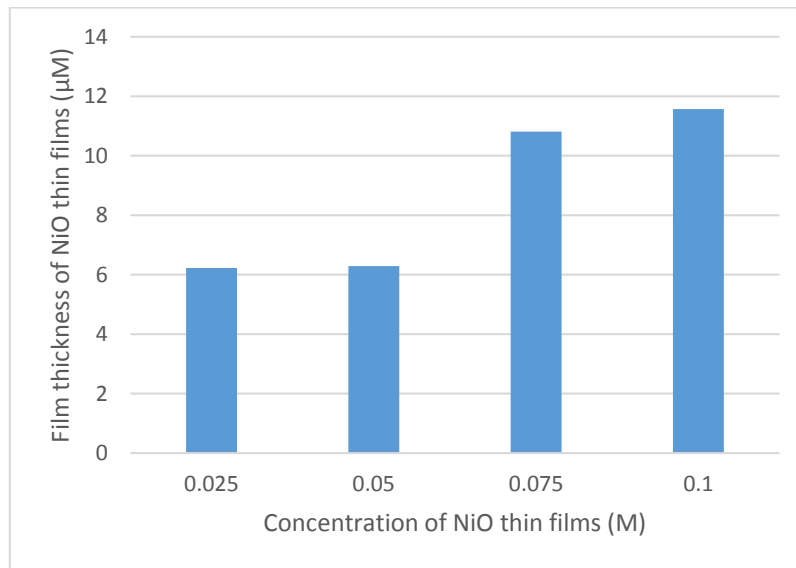

Figure 5. Film thickness of NiO thin films using weight difference method

There was no disparity between the SEM cross sectional profiling and the film thickness obtained using the weight difference. Film thickness increases as precursor concentration increases. This is an improvement on previous study results [48]. This improvement may be as a result of accumulation of deposited NiO on the substrate. This was collaborated by the EDX results. The thickness of the NiO film was controlled by keeping the deposition parameters constant. The NiO thin film average thickness was between 6.277 μm and 11.57 μm.

Structural Studies

The phase and the preferred orientation of the deposited nanostructured NiO films were determined using an x-ray diffractometer. Figure 6 gives the XRD patterns of the deposited nanostructured NiO films at different precursor concentrations. The patterns have peak diffractions at ($2\theta = 37$ º and 43 º) for the (1 1 1) and (2 0 0) planes respectively and 64 º for the (2 2 0) plane for 0.1 M. The XRD analysis confirms Bunsenite which corresponds to the JCPDS card: 04- 0835 for

Nickel oxide [49]. The highest intensity was recorded for the (1 1 1) plane with a strong peak of $2\theta = 37$ ° for precursor solutions of 0.05 M, 0.075 M and 0.1 M which is an improvement on Bakr et al. [50]. This could be due to an increase in grain growth caused by greater thickness. It can also be due to an increase in crystallinity as the concentration of the precursor solution increases. These results confirm the polycrystalline with cubic crystalline structures of deposited NiO film. Balu et al. [51] also observed polycrystalline with cubic structures when they varied concentrations of NiO films using SPT with a perfume atomizer but this seemed to have more intensity. The lower intensity peak of (2 0 0) increased gradually as the precursor solution increased from 0.05 M to 0.1 M with emergence of a third peak of (2 2 0) for 0.1 M. The average crystallite size was obtained using the Debye-Scherrer formula [52-53] in Equation (3).
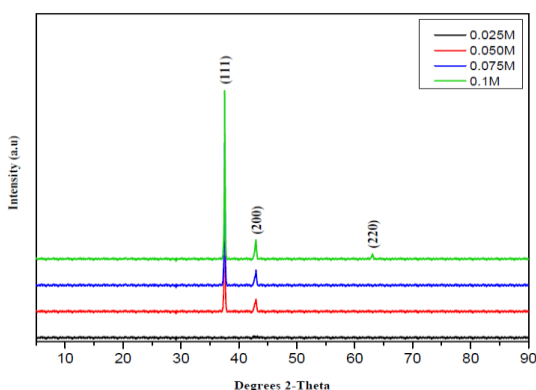

Figure 6. XRD patterns of nanostructured NiO films for various precursor concentrations

$$D = \frac{k\lambda}{\beta \cos\theta} \qquad (3)$$

Where B is full width at half maximum (FWHM) peak intensity (in Radian), λ is wavelength, θ represent Bragg's diffraction angle and k is 0.89 respectively.

The lattice constant was found to be 4.1905 Å, 4.1856 Å, 4.1852 Å, 4.1850 Å for 0.025 M to 0.1 M respectively. This agrees with the standard lattice constant of NiO film value of 4.176 Å [54].

Micro strain was produced through growth of thin film and was calculated using the formula in Equation (4) [55].

$$\delta = \frac{d_{ASTM} - d_{XRD}}{d_{ASTM}} \times 100 \qquad (4)$$

Where d is the lattice constant and δ is the micro strain.

A plot of NiO film micro strain against precursor solution is shown in Fig. 7. It shows that there is an increase in micro strain as precursor concentration increases. Micro strain represents compression as seen in Table 2 which gives detailed results of micro strain, lattice constants and 2θ values for deposited NiO films for precursor solution concentrations of 0.025 M to 0.1 M.

Table 2. Calculated parameters from XRD data

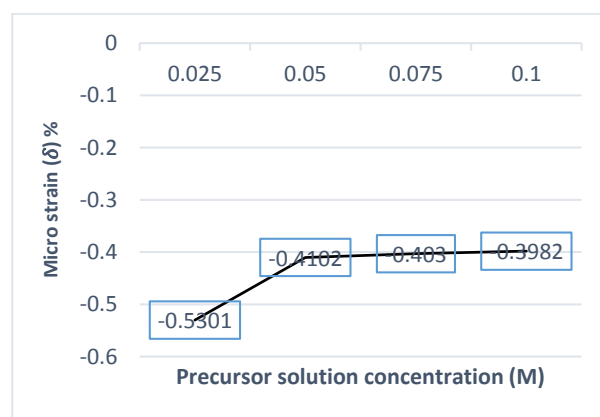| Parameter		0.025	0.05M	0.075	0.1M
2θ	hkl		37	37	37
	(1 1 1)				
	(2 0 0)	x	43	43	43
	(2 2 0)	x	X	X	63
Lattice constant d (Å)	recorded XRD	4.1905	4.1855	4.1852	4.1850
	ASTM	4.1684	4.1684	4.1684	4.1684
Micro strain (δ) %		-0.5301	-0.4102	-0.4030	-0.3982

Figure 7. Graph of micro strain against precursor solution concentration for NiO films

Optical properties

Figure 8 represents measurements of transmittance and wavelength for deposited NiO films at various precursor solution concentrations. Transmittance decreases from 80 % to 71 % as precursor solution concentration increases (0.025 M to 0.1 M). This may be ascribed to the increased value of NiO thickness and absorbance. The absorption edge in thicker films was less sharp. This occurred because as precursor concentration increases there is bigger cluster of deposited films causing the scattered radiation to be more pronounced because of surface roughness [56]. These results exceeded previous reported values [57-58].
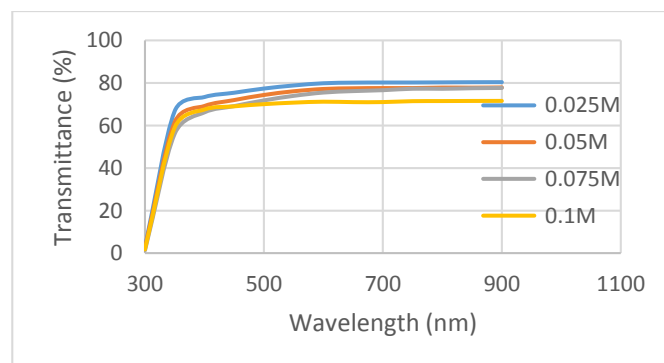

Figure 8. Plot of transmittance against wavelength of varied NiO film molarity

Absorption coefficient, α was obtained using Equation (5) [59].

$$\alpha = (2.303 \times A) / t \qquad (5)$$

Where t is film thickness and A is absorbance. Optical absorption is related with optical energy band gap as expressed in Equation (6) [60-61].

$$\alpha^2 = C \left(h\upsilon - E_g \right) \qquad (6)$$

Where C has constant value, h denotes Planck's constant, υ represent incidence light frequency, and E_g denotes optical energy band gap.
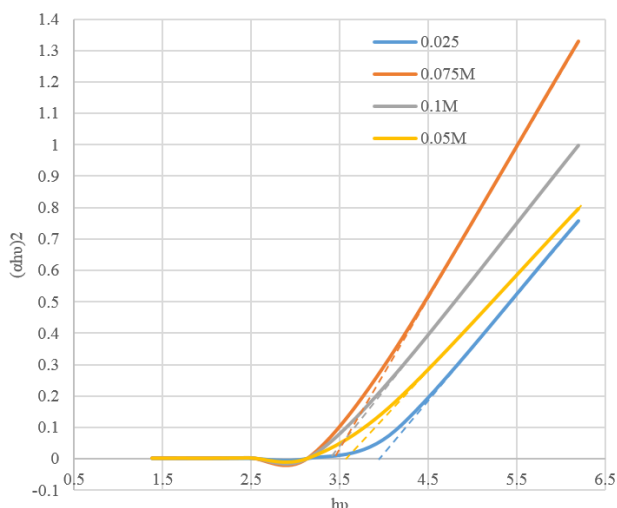

Figure 9. Graph of $(\alpha h\upsilon)^2$ against hυ for NiO films

Figure 9 shows a graph of $(\alpha h\upsilon)^2$ against hυ for NiO film spray deposited at different precursor concentrations. Extrapolation of the linear line of the graph to hυ axis for $(\alpha h\upsilon)^2 = 0$ gives the optical band gap. A decrease in slope of the plot is also observed as precursor concentration increases. A shift towards lower energy is observed according to the value of the optical band gap. This reduction is attributed to the Moss-Burstein shift [62-63]. Optical energy band gaps are: 3.94 eV, 3.56 eV, 3.44 eV and 3.38 eV for 0.025 M, 0.05 M, 0.075 M and 0.1 M respectively. This gives a better optical band gap than existing reported values [64]. This may be ascribed to crystallite size increment as precursor concentration decreases [65]. A quantum size effect may be responsible for the large value of the band gap of NiO film [66]. Careful and well optimized deposition parameters also helped in obtaining better optical band gaps.
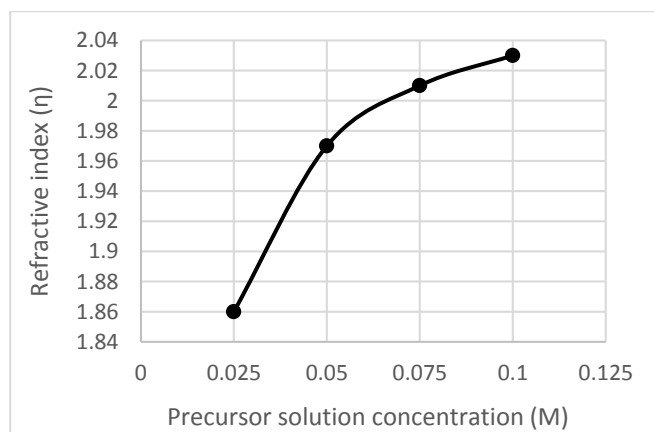

Figure 10. Variation of refractive index with precursor solution concentration of NiO films

The refractive index of deposited films, shown in Fig. 10, was calculated using the relation between the refractive index and the optical band gap as shown in Equation 7 [67].

$$\eta = \sqrt{(12.417 / (E_g - 0.365)} \qquad (7)$$

Where η is refractive index and E_g is optical band gap. The refractive indices were found to be 1.86, 1.97, 2.01 and 2.03 for precursor solutions of 0.025 M, 0.05 M, 0.075 M and 0.1 M respectively. This is an improvement on reported values by Sriram and Thayumanavan [68].

CONCLUSION

This study showed successful spray deposition of nanostructured NiO films using nickel acetate on glass substrate. The effect of varying precursor concentrations of NiO films in terms of elemental, morphological and structural properties were studied. In terms of Elemental and morphology properties, surface morphology showed an increasingly grainier surface as the molarity increased. Elemental composition confirmed the presence of the Ni and O elements in NiO films. Oxygen concentration decreased as precursor concentration increased. It was observed that the film thickness increased as the precursor solution increased from 0.025 M to 0.1 M with an average thickness range of 10 μm and 21μm respectively.

XRD patterns showed that the 0.025 M concentration has an amorphous structure while the 0.05 M to 0.1 M concentrations have a polycrystalline cubic structure. Intensity of NiO films increased with increased molarity. Preferred orientation was along the (1 1 1) peak. The patterns had peak diffraction at (2θ = 37 º, and 43 º) for the (1 1 1) and (2 0 0) planes respectively and 64 º for the (2 2 0) plane for 0.1 M. The lattice constant decreased from 4.1905 Å to 4.1850 Å for 0.025 M to 0.1 M which correlated with the 4.176 Å standard lattice constant of NiO. Micro strain of films showed compression and increases with precursor concentration.

Transmittance reduced as precursor concentration increased. Transmittance decreased from about 80 % to 71 % as concentration increased. Optical band gap varied from 3.94 eV

to 3.38 eV as concentration increased. This study produced better optical band gaps than existing literature. These new results were as a result of optimization of the deposition parameters. Therefore, varying precursor solution concentration has an effect on properties of nanostructured NiO thin film. Based on the result obtained, the prepared NiO thin film sample can be used as an absorber layer of a solar cell. This optimized result may be the answer to low cost, durable yet efficient solar cell fabrication and research in developing countries.

ACKNOWLEDGEMENTS

REFERENCES

[1]   Grätzel, M., 2004, "Mesoscopic Solar Cells for Electricity and Hydrogen Production from Sunlight," Chem. Lett., 34(1), pp. 8-13.

[2]   Lubega, W. N., and Farid. A. M., 2014, "Quantitative Engineering Systems Modeling and Analysis of the Energy-Water Nexus," Appl. Energy,135, pp. 142-157.

[3]   Shyu, C.-W., 2014, "Ensuring Access to Electricity and Minimum Basic Electricity Needs as a Goal for the Post-MDG Development Agenda after 2015," Energy Sustainable Dev., 19, 29-38.

[4]   International Energy Agency, United Nations Development Programme and United Nations Industrial Development Organisation, 2010, "Energy Poverty: How to make Modern Energy Access Universal? Special Early Excerpt of the World Energy Outlook 2010 for the UN General Assembly on the Millennium Development Goals. Paris: Organization for Economic Co-Operation and Development/International Energy Agency. Energy Modern Energy Services in Brazil, 269.

[5]   International Energy Agency, 2013, World Energy Outlook Special Report. Paris:). Retrieved from: https://www.iea.org/publications/freepublications/pu blication/SoutheastAsiaEnergyOutlook_ WEO2013SpecialReport. pdf.

[6]   REN21., 2015, Renewables 2015 Global Status Report. Paris: REN21 Secretariat.

[7]   Ellabban, O., Abu-Rub, H., and Blaabjerg, F., 2014, "Renewable Energy Resources: Current Status, Future Prospects and their Enabling Technology," Renewable Sustainable Energy Rev., 39, pp.748-764.

[8]   Emodi, N., and Yusuf, S., 2015, Improving Electricity Access in Nigeria: Obstacles and the Way Forward. Int. J. Energy Economics Policy, 5(1), pp. 335-351.

[9]   Hussein, A. K., 2015, "Applications of

Nanotechnology in Renewable Energies—A Comprehensive Overview and Understanding," Renewable Sustainable Energy Rev., 42, pp. 460-476.

[10]   Lewis, N. S., 2007, "Toward Cost-Effective Solar Energy Use," Science, 315, pp. 798-801.

[11]   Bustamante, M. L., and Gaustad. G., 2014, "Challenges in Assessment of Clean Energy Supply-Chains Based on Byproduct Minerals: A Case Study of Tellurium use in Thin Film Photovoltaics," Appl. Energy, 123, pp. 397-414.

[12]   Menoufi, K., Chemisana D., and Rosell. J. I., 2013, "Life Cycle Assessment of a Building Integrated Concentrated Photovoltaic Scheme" Appl. Energy, 111, pp. 505-514.

[13]   Gardner, G., 2008, Alternative Energy and Nanotechnology. Publ. Commun. Sci. Technol.

[14]   Green, M. A., 1982, Solar Cells: Operating Principles, Technology, and System Applications. Prentice-Hall, Englewood Cliffs, NJ.

[15]   Eslamian, M., 2014, "Spray-On Thin Film PV Solar Cells: Advances, Potentials and Challenges," Coat., 4, pp. 60-84.

[16]   Serrano, E., Rus, G., and Garcia-Martinez J., 2009, "Nanotechnology for Sustainable Energy," Renewable Sustainable Energy Rev., 13, pp. 2373-2384.

[17]   Bankole, M., Tijani, J. O., Mohammed, I., and Abdulkareem, A., 2014, "A Review on Nanotechnology as a Tool of Change in Nigeria," Sci. Res. Essays, 9, 213-223.

[18]   Joshi, S., Mudigere, M., Krishnamurthy, L., Shekar, G., 2014, "Growth and Morphological Studies of NiO/CuO/ZnO Based Nanostructured Thin Films for Photovoltaic Applications," Chem. Pap., 68:1584-1592.

[19]   Rahal, A., Benhaoua, A., Jlassi, M., and Benhaoua, B., 2015, "Structural, Optical and Electrical Properties Studies of Ultrasonically Deposited Tin oxide (SnO$_2$) Thin Films with Different Substrate Temperatures," Superlattices Microstruct., 86, pp. 403-411.

[20]   Zhang, W., Ding, S., Yang, Z., Liu, A., Qian ,Y., Tang, S., and Yang, S., 2006, "Growth of novel Nanostructured Copper Oxide (CuO) Films on Copper Foil," J. Cryst. Growth, 291, pp. 479-484.

[21]   Shaikh, S. K., Inamdar, S. I., Ganbavle, V. V., and Rajpure, K. Y., 2016," Chemical Bath Deposited ZnO Thin Film Based UV Photoconductive Detector," J. Alloys Compd., 664, pp. 242-249.

[22]   Drevet, R, Legros C, Bérardan D, Ribot P, Dragoé D, Cannizzo C., and Andrieux M., 2015, "Metal Organic Precursor Effect on the Properties of SnO 2 Thin Films Deposited by MOCVD Technique for Electrochemical Applications," Surf. Coat. Technol.,

271, pp. 234-241.

[23] Soonmin, H., 2016 "Preparation and Characterization of Nickel Oxide Thin Films: A Review," Int. J. Appl. Chem., 12, pp. 87-93.

[24] Nam, W. J., Gray, Z., Stayancho, J., Plotnikov, V., Kwon, D., Waggoner, S., et al., 2015, "ALD NiO Thin Films as a Hole Transport-Electron Blocking Layer Material for Photo-Detector and Solar Cell Devices," ECS Meeting Abstracts, 66, pp. 275-279.

[25] Park, N., Sun, K., Sun, Z., Jing, Y., and Wang, D., 2013, "High Efficiency NiO/ZnO Heterojunction UV Photodiode by Sol-Gel Processing," J. Mater. Chem. C, 1, pp. 7333-7338.

[26] Li, C., and Zhao Z., 2010, "Preparation and Characterization of Nickel Oxide Thin Films by a Simple Two-Step Method," In Vacuum Electron Sources Conference and Nanocarbon (IVESC), 2010 8th International, pp. 648-649.

[27] Wu, C-C., and Yang, C-F., 2015, "Effect of Annealing Temperature on the Characteristics of the Modified Spray Deposited Li-Doped NiO Films and their Applications in Transparent Heterojunction Diode," Sol. Energy. Mater. Sol. Cells, 132, pp. 492-498.

[28] Zhu, Z., Bai, Y., Zhang, T., Liu, Z., Long, X., Wei, Z, et al., 2014, "High-Performance Hole-Extraction Layer of Sol-Gel-Processed NiO Nanocrystals for Inverted Planar Perovskite Solar Cells," Angewandte Chemie, 126, pp. 12779-12783.

[29] Magaña, C. R., Acosta, D. R., Martínez, A. I., Ortega, J. M., 2006, "Electrochemically Induced Electrochromic Properties in Nickel Thin Films Deposited by DC Magnetron Sputtering," Sol. Energy, 80, pp. 161-169.

[30] Su, S. Liu, T., Wang, Y., Chen, X., Wang, J., and Chen, J,. 2014, "Performance Optimization Analyses and Parametric Design Criteria of a Dye-Sensitized Solar Cell Thermoelectric Hybrid Device," Appl. Energy, 120, pp. 16-22.

[31] Wang, X., Li, H., Liu, Y., Zhao, W., Liang, C., Huang, H., Mo, D., Liu, Z., Yu, X. and Deng, Y., 2012, "Hydrothermal Synthesis of Well-Aligned Hierarchical Tio$_2$ Tubular Macrochannel Arrays with Large Surface Area for High Performance Dye-Sensitized Solar Cells," Appl. Energy, 99, pp. 198-205.

[32] Kim, H-J, and Lee, J-H., 2014, "Highly Sensitive and Selective Gas Sensors Using P-Type Oxide Semiconductors: Overview," Sens. Actuators B: Chem., 192, pp. 607-627.

[33] Subramanian, B., Ibrahim, M. M., Senthilkumar, V., Murali, K., Vidhya, V., Sanjeeviraja, C., and Jayachandran, M., 2008, "Optoelectronic and Electrochemical Properties of Nickel Oxide (Nio) Films Deposited by DC Reactive Magnetron

Sputtering," Physica B: Condens. Matter, 403, pp. 4104-4110.

[34] Keraudy, J., García Molleja, J., Ferrec, A., Corraze, B., Richard-Plouet, M., Goullet, A., et al., 2015, "Structural, Morphological and Electrical Properties of Nickel Oxide Thin Films Deposited by Reactive Sputtering," Appl. Surf. Sci, 357, Part A, pp. 838-844.

[35] Jlassi, M., Sta, I., Hajji, M., and Ezzaouia, H., 2014, "Optical and Electrical Properties of Nickel Oxide Thin Films Synthesized by Sol-Gel Spin Coating," Mater. Sci. Semicond. Process, 21, pp. 7-13.

[36] El-Nahass, M. M., Emam-Ismail, M., and El-Hagary, M., 2015, "Structural, Optical and Dispersion Energy Parameters of Nickel Oxide Nanocrystalline Thin Films Prepared by Electron Beam Deposition Technique," J. Alloys Compd., 646, pp. 937-945.

[37] Wang, H., Wang, Y., and Wang, X., 2012, "Pulsed Laser Deposition of the Porous Nickel Oxide Thin Film at Room Temperature for High-Rate Pseudocapacitive Energy Storage," Electrochem. Commun., 18, pp. 92-95.

[38] Vidales-Hurtado, M. A., and Mendoza-Galván, A., 2008, "Electrochromism in Nickel Oxide-Based Thin Films Obtained by Chemical Bath Deposition," Solid State Ionics, 179, pp. 2065-2068.

[39] Gowthami, V., Perumal, P., Sivakumar, R., and Sanjeeviraja, C., 2014, "Structural and Optical Studies on Nickel Oxide Thin Film Prepared by Nebulizer Spray Technique," Physica B: Condens. Matter, 452, pp. 1-6.

[40] Patil, P. S., 1999, "Versatility of Chemical Spray Pyrolysis Technique," Mater. Chem. Phys., 59, pp. 185-198.

[41] Faraj, M. G., 2015, "Effect of Aqueous Solution Molarity on the Structural and Electrical Properties of Spray Pyrolysed Lead Sulfide (PbS) Thin Films," Int. Lett. Chem. Phys. Astron., 57, pp. 122.

[42] Ukoba, K. O, Eloka-Eboka, A. C., and Inambao, F. L., 2017, "Review of Nanostructured Nio Thin Film Deposition Using the Spray Pyrolysis Technique," Renewable Sustainable Energy Rev. In Press., http://dx.doi.org/10.1016/j.rser.2017.10.041

[43] Bari, R., Patil, S., and Bari, A., 2013, "Effect of Molarity of Precursor Solution on Physical, Structural, Microstructural and Electrical Properties of Nanocrystalline Zno Thin Films," Mater. Technol., 28, pp. 214-220.

[44] Saadati, F., Grayeli, A., and Savaloni, H., 2010, "Dependence of the Optical Properties of Nio Thin Films on Film Thickness and Nano-Structure," J. Theor. Appl. Phy., 4, pp. 22-26.

[45] Reguig, B., Regragui, M., Morsli, M., Khelil, A., Addou, M., and Bernede, J., 2006, "Effect of the Precursor Solution Concentration on the Nio Thin

Film Properties Deposited by Spray Pyrolysis," Sol. Energy Mater. Sol. Cells, 90, pp. 1381-1392.

[46] de Jong, B. H. W. S., 1989, Glass in Ullman's Encyclopedia of Industrial Chemistry, 5th ed. vol. A12, VCH Publishers, Weinheim, Germany, pp. 365-432.

[47] Godse, P., Sakhare, R., Pawar, S., Chougule, M., Sen, S., Joshi, P., et al., 2011, "Effect of Annealing on Structural, Morphological, Electrical and Optical Studies of Nickel Oxide Thin Films," J. Surf. Eng. Mater. Adv. Technol., 1, pp. 35.

[48] Boyraz, C., and Urfa, Y., 2015, "Effect of Solution Molarity on Microstructural and Optical Properties of CdCr 2 S 4 thin films," Mater. Sci. Semicond. Process., 36, pp. 1-6.

[49] Gabal, M., 2003, "Non-Isothermal Decomposition of NiC_2O_4–FeC_2O_4 Mixture Aiming at the Production of NiFe 2 O 4," J. Phys. Chem. Solids, 64, pp. 1375-1385.

[50] Bakr, N. A., Salman, S. A., and Shano, A. M., 2015, "Effect of Co Doping on Structural and Optical Properties of NiO Thin Films Prepared By Chemical Spray Pyrolysis Method," Int. Lett. Chem. Phys. Astron., 41, pp. 15-30.

[51] Balu, A., Nagarethinam, V., Suganya, M., Arunkumar, N., and Selvan, G., 2012, "Effect of Solution Concentration on the Structural, Optical and Electrical Properties of SILAR Deposited CdO thin films," J. Electron. Devices, 2, pp. 739-749.

[52] Scherrer, P., Nachr, G., 1918, "Derivation of Crystallite Size," OH HO OH OH OH O OH.

[53] Barrett, C., and Massalski, T., 1980, Structure of Metals, Pergamon Press, Oxford.

[54] Pistorius, C. W. F. T., 1963, "Some Phase Relations in the System COO-SiOerO. NiO-SiOz-Hzo and ZnO-SiOrHiO to High Pressures and Temperatures," Neues Jahrb Mineral Monatsh, pp. 30-57.

[55] Mohammad, A. J., 2006, "Studying the Effect of Molarity on the Physical and Sensing Properties of Zinc Oxide Thin Films Prepared by Spray Pyrolysis Technique," PhD thesis, Applied Science Dep. University of Technology, Baghdad.

[56] Balu, A., Nagarethinam, V., Arunkumar, N., and Suganya, M., 2012, "Nanocrystalline NiO Thin Films Prepared by A Low Cost Simplified Spray Technique Using Perfume Atomizer," J. Electron. Devices, 13, pp. 920-930.

[57] Ismail, R. A., Ghafori, S. A., and Kadhim, G. A., 2013, "Preparation and Characterization of Nanostructured Nickel Oxide Thin Films By Spray Pyrolysis," Appl. Nanosci. 3, pp. 509-514.

[58] Fadheela, H. O., 2015, "Structural and Optical Characterization of Nickel Oxide Thin Films Prepared by Spray Pyrolysis Technique," Eng. Tech. J., 33, pp. 10.

[59] Barman, J., Sarma, K., Sarma, M., and Sarma, K., 2008, "Structural and Optical Studies of chemically Prepared Cds Nanocrystalline Thin Films," Indian J. Pure Appl. Phys., 46, pp. 339-343.

[60] Ezema, F., Ekwealor, A., and Osuji, R., 2006, "Effect of Thermal Annealing on the Band GAP and Optical Properties of Chemical Bath Deposited Znse Thin Films," Turk. J. Phys., 30, pp. 157-163.

[61] Estrella, V., Nair, M., and Nair, P., 2003, "Semiconducting Cu3BiS3 Thin Films Formed by the Solid-State Reaction of CuS and Bismuth Thin Films," Semicond. Sci. Technol., 18, pp. 190.

[62] Burstein, E., 1954, "Anomalous Optical Absorption Limit in InSb," Phys. Rev., 93, pp. 632.

[63] Moss, T., 1954, "The Interpretation of the Properties of Indium Antimonide," Proc. Phys. Soc. Section B., 67, pp. 775.

[64] Boschloo, G., and Hagfeldt, A., 2001, "Spectroelectrochemistry of Nanostructured NiO," J. Phys. Chem. B., 105, pp. 3039-3044.

[65] Makhlouf, S., Kassem, M., and Abedulrahim, M., 2010, "Crystallite Size Dependent Optical Properties of Nanostructured Nio Films," J. Optoelectron. Adv. Mater., 4, pp. 1562.

[66] Romero, R., Martin, F., Ramos-Barrado, J., and Leinen, D., 2010, "Synthesis and Characterization of Nanostructured Nickel Oxide Thin Films Prepared with Chemical Spray Pyrolysis," Thin Solid Films, 518, pp. 4499-4502.

[67] Reddy, R., Aharnmed, Y. N., Azeem, P. A., Gopal, K. R., Devi, B. S., and Rao, T., 2003, "Dependence of Physical Parameters of Compound Semiconductors on Refractive Index," Defence Sci. J., 53, pp. 239.

[68] Sriram, S., and Thayumanavan, A., 2013, "Structural, Optical and Electrical Properties of NiO Thin Films Prepared by Low Cost Spray Pyrolysis Technique," Int. J. Mater. Sci. Eng., 1, pp. 118-21.

[69] Chen, Z., Zhang, X.-d. Fang, J. Liang, J.-h. Liang, X.-j. Sun, J. Zhang, D.-k. Wang, N. Zhao H.-x. and Chen, X.-l., 2014, "Enhancement in Electrical Performance of Thin-Film Silicon Solar Cells Based on a Micro- and Nano-Textured Zinc Oxide Electrode," Applied Energy; 135, pp. 158-164.